ISSN: 2231-3656

International Journal of Pharmacy and Industrial Research (IJPIR)

IJPIR |Vol. 16 | Issue 4 | Oct – Dec 2026

www.ijpir.com

DOI: https://doi.org/10.61096/ijpir.v16.iss4.2026.1106-1117

Formulation and *In-Vitro* Evaluation of Nilotinib and Quercetin Fused Nanoparticles for Enhanced Therapy of Myeloid Leukemia

Sathish P[1,3*], Shalini S[1,3], Krishnamoorthy B [1,3], Perumal P[2,3]

[1] *Department of Pharmaceutics, JKK Munirajah Institute of Health Sciences College of Pharmacy, Erode, Tamil Nadu, India*

[2] *Department of Pharmaceutical Chemistry, JKK Munirajah Institute of Health Sciences College of Pharmacy, Erode, Tamil Nadu, India*

[3] *Affiliated to The Tamil Nadu Dr. M.G.R. Medical University, Chennai, Tamil Nadu, India*

*Corresponding author: **Sathish P**
Email: bpharmsathiszz03@gmail.com

Published on:

20.11.2026

Published by:

Futuristic Publications

2026| All rights reserved.

Creative Commons Attribution 4.0 International License.

Abstract

Background: Nilotinib is a BCR-ABL tyrosine kinase inhibitor used in chronic myeloid leukemia (CML), but its poor aqueous solubility may limit formulation performance. Quercetin is a flavonoid with reported anticancer activity and similarly limited aqueous solubility. This study investigated co-loading of nilotinib and quercetin into solid lipid nanoparticles (SLNs) and in-vitro performance.

Methods: Preformulation studies included melting point, solvent solubility, UV calibration and FTIR compatibility. Twelve batches (T1-T12) were prepared by hot homogenization followed by probe ultrasonication using glyceryl monostearate (GMO; 4% or 6%) with Tween 80 or Span 20 (1-2%). The formulations were evaluated for physical appearance, entrapment efficiency, nilotinib content, in-vitro release, particle size, polydispersity index (PDI), zeta potential, morphology and cytotoxicity in K562 cells using an MTT assay.

Results: Tween 80 batches (T1-T6) remained dispersed, whereas Span 20 batches (T7-T12) underwent phase separation. T5 (6% GMO and 1.5% Tween 80) showed the highest reported entrapment efficiency (86%) and the most prolonged release, reaching 99.92% for nilotinib and 99.17% for quercetin at 30 h. The optimized batch had a particle size of 278 nm, PDI of 0.031 and zeta potential of −32 mV. The reported IC50 values in K562 cells were 4.40, 36.15, 3.80 and 3.03 µg/mL for nilotinib, quercetin, free combination and combination SLN, respectively.

Conclusion: The co-loaded T5 formulation demonstrated sustained in-vitro release and the lowest reported IC50 among the tested treatments. The findings are preliminary; replicate-based cytotoxicity, blank-carrier controls, storage stability and in-vivo studies are required before drawing translational conclusions.

Keywords: Nilotinib; Quercetin; Solid lipid nanoparticles; Chronic myeloid leukemia; K562 cells; Co-delivery.

1. INTRODUCTION

Chronic myeloid leukemia (CML) is a clonal myeloproliferative neoplasm associated with the Philadelphia chromosome, resulting from a reciprocal translocation between chromosomes 9 and 22. This

rearrangement generates the BCR: ABL1 fusion gene, which encodes a constitutively active tyrosine kinase that promotes abnormal myeloid-cell proliferation and survival. Targeting BCR::ABL1 has transformed the treatment of CML.

Nilotinib is a second-generation BCR: ABL1 tyrosine kinase inhibitor used in CML. It has demonstrated activity in patients with resistance or intolerance to imatinib and has been evaluated as a frontline treatment. Despite its therapeutic activity, nilotinib has poor aqueous solubility and is associated with clinically important adverse effects, including QT-interval prolongation and metabolic effects. Formulation strategies that improve its pharmaceutical performance are therefore of interest.

Quercetin is a naturally occurring flavonoid found in several plant-derived foods. Experimental studies have reported antioxidant and anticancer-related effects, including modulation of apoptosis, cell-cycle progression and cancer-associated signalling. Its limited aqueous solubility and bioavailability, however, constrain its pharmaceutical application. Co-delivery with nilotinib may provide a platform to investigate the combined in-vitro effects of these agents.

Solid lipid nanoparticles are colloidal carriers composed of lipids that remain solid at room and physiological temperatures and are stabilized by surfactants. SLNs can incorporate lipophilic compounds and may modify their release characteristics. Their composition, lipid content and surfactant selection influence particle formation, dispersion stability, drug entrapment and release.

The present study was designed to formulate Nilotinib-quercetin co-loaded SLNs using hot homogenization and ultrasonication, compare Tween 80 and Span 20 as stabilizers, identify a lead batch using the reported physicochemical and release results, and evaluate the in-vitro cytotoxic response in K562 cells.

1.1 Study rationale and objectives

The formulation rationale was based on the limited aqueous solubility of both drug candidates and the potential of a lipid-based carrier to incorporate lipophilic compounds. The work compared two surfactants and two GMO levels to examine their influence on the preparation outcome.

The objectives were:

- To characterize nilotinib and quercetin by melting-point and solubility studies.
- To construct UV calibration curves for nilotinib and quercetin and assess drug-excipient compatibility by FTIR.
- To prepare twelve nilotinib-quercetin SLN batches using different GMO and surfactant concentrations.
- To evaluate physical appearance, entrapment efficiency, nilotinib content, in-vitro release, particle size, PDI, zeta potential and surface morphology.
- To compare the in-vitro cytotoxic response of nilotinib, quercetin, their free combination and the co-loaded SLN in K562 cells.

1.2 Experimental overview

The experimental sequence comprised preformulation characterization, preparation of the twelve trial batches, selection of the most suitable Tween 80-stabilized dispersion, physicochemical characterization of the selected batch, and an MTT-based cytotoxicity assessment. The study was conducted as an in-vitro formulation investigation; no animal or clinical evaluation was reported.

The disease model used in the manuscript is CML and the cell line reported is K562. Accordingly, the findings are discussed in the context of BCR: ABL1-positive CML research and are not generalized to acute myeloid leukemia.

2. MATERIALS AND METHODS

2.1 Materials

Nilotinib was obtained from Dhamtech Private Limited, Mumbai, and Quercetin from Nalinc Pharmaceuticals Limited, Mumbai. Glyceryl monostearate (GMO), Tween 80 and Span 20 were used as lipid and surfactant components. Methanol was obtained from EID Parry, India. The research also lists chloroform, dimethyl sulfoxide (DMSO), ethanol, hydrochloric acid and distilled water as solvents or media used during the experimental procedures.

2.2 Equipment

Equipment	Manufacturer / model reported
Analytical balance	Sartorius BT224, Germany
Orbital shaker	Neolab
HPLC system	Thermo Scientific
FTIR spectrophotometer	Shimadzu
Dissolution apparatus	Lab India Disso 800
Scanning electron microscope	JEOL / Hitachi instruments reported in research
Particle-size / zeta-potential analyzer	Malvern / Anton Paar Litesizer 500 (as reported)
Digital pH meter	Wensar

2.3 Preparation of Nilotinib-Quercetin SLNs

Nilotinib (5 mg), quercetin (10 mg) and GMO were dissolved in a chloroform-DMSO mixture (1:2, v/v). The organic solvents were removed under vacuum using a rotary evaporator. An aqueous phase containing Tween 80 or Span 20 in distilled water (30 mL) was heated to 70 °C and added to the lipid phase. The system was maintained above the lipid melting temperature. The resulting dispersion was homogenized at 2500 rpm and 70 °C for 30 min, followed by probe ultrasonication for 25 min. The hot nanoemulsion was cooled to room temperature and stored at 4 °C.

T1-T6 contained Tween 80 at 1%, 1.5% or 2% with GMO at 4% or 6%; T7-T12 used the corresponding Span 20 concentrations. Each batch contained nilotinib 5 mg and quercetin 10 mg.

2.4 Formulation design

Batch	Nilotinib (mg)	Quercetin (mg)	GMO (%)	Tween 80 (%)	Span 20 (%)
T1	5	10	4	1	-
T2	5	10	4	1.5	-
T3	5	10	4	2	-
T4	5	10	6	1	-
T5	5	10	6	1.5	-
T6	5	10	6	2	-
T7	5	10	4	-	1
T8	5	10	4	-	1.5
T9	5	10	4	-	2
T10	5	10	6	-	1
T11	5	10	6	-	1.5
T12	5	10	6	-	2

2.5 Preformulation and analytical procedures

Melting points were determined by the open-capillary method. Solubility was assessed by dispersing 1 mg of each drug in 10 mL of distilled water, methanol, ethanol, DMSO or 0.1 N HCl (pH 1.2):ethanol (3:1,

v/v), followed by 24 h of shaking, filtration and UV analysis. The research describes three independent determinations for the solubility assessment.

UV calibration curves were prepared at 263 nm for nilotinib and 376 nm for quercetin. FTIR spectra were recorded from 400 to 4000 cm^{-1} at 4 cm^{-1} resolution using the KBr-disc method. Individual drug and excipient spectra were compared with the physical mixture for changes in characteristic bands.

2.6 Entrapment efficiency and drug content

For entrapment assessment, the dispersion was centrifuged at 20,000 rpm for 1 h at 4 °C. The supernatant was filtered through a 0.22 µm membrane, diluted with 0.1 N HCl and analyzed at 263 nm to quantify unencapsulated nilotinib. The reported entrapment-efficiency values are reproduced from the research results. Drug content was assessed by dissolving an aliquot of the dispersion in 0.1 N HCl:ethanol (3:1, v/v) and measuring nilotinib at 263 nm.

2.7 In-vitro release study

In-vitro release was studied at 37 °C using a dialysis bag with a 10 kDa molecular-weight cut-off. A sample equivalent to 3 mg drug was placed in the dialysis bag and immersed in 200 mL of 0.1 N HCl: Ethanol (3:1, v/v), with stirring at 100 rpm. Samples were withdrawn at predetermined intervals for up to 48 h and replaced with fresh medium to maintain sink conditions. Nilotinib and quercetin were quantified at 263 nm and 376 nm, respectively.

2.8 Particle size, PDI and zeta potential

Particle size, PDI and zeta potential were measured by dynamic light scattering/electrophoretic light scattering using an Anton Paar Litesizer 500 after appropriate dilution with distilled water. The thesis reports a particle size of 278 nm and PDI of 0.031. The zeta-potential instrument output on thesis page 69 records −0.032 V (−32 mV).

2.9 Surface morphology

The SLN dispersion was mounted on a metal stub using double-sided adhesive tape, coated with a thin gold-palladium layer and examined by scanning electron microscopy at an accelerating voltage of 5 kV. The thesis presents SEM images at ×1000 magnification.

2.10 In-vitro cytotoxicity

K562 cells were exposed to nilotinib, quercetin, their free combination or the co-loaded SLN over 5-40 µg/mL. Cells were maintained in RPMI-1640 complete medium at 37 °C and 5% CO_2. Viability was assessed by the MTT assay, and IC50 values were reported from the concentration-response data.

3. RESULTS

3.1 Preformulation characterization

Table 1. Melting point and qualitative solubility profile of Nilotinib and Quercetin.

Parameter	Nilotinib	Quercetin
Melting point	258 °C	317 °C
Distilled water	Insoluble	Poorly soluble
Methanol	Sparingly soluble	Soluble
Ethanol	Sparingly soluble	Soluble
DMSO	Soluble	Soluble
0.1 N HCl: Ethanol (3:1)	Soluble	Soluble

Nilotinib was reported while it was soluble in DMSO and the acid-ethanol mixture. Quercetin was poorly soluble in water and soluble in the organic solvents examined. The acid-ethanol mixture was used as the analytical medium for drug-content and release measurements.

3.2 UV calibration

The nilotinib calibration curve was linear over 2-10 µg/mL, with the reported regression equation y = 0.066x + 0.0023 (R^2 = 0.9984). The quercetin calibration curve was linear over 10-60 µg/mL, with y = 0.041x + 0.0136 (R^2 = 0.9968).

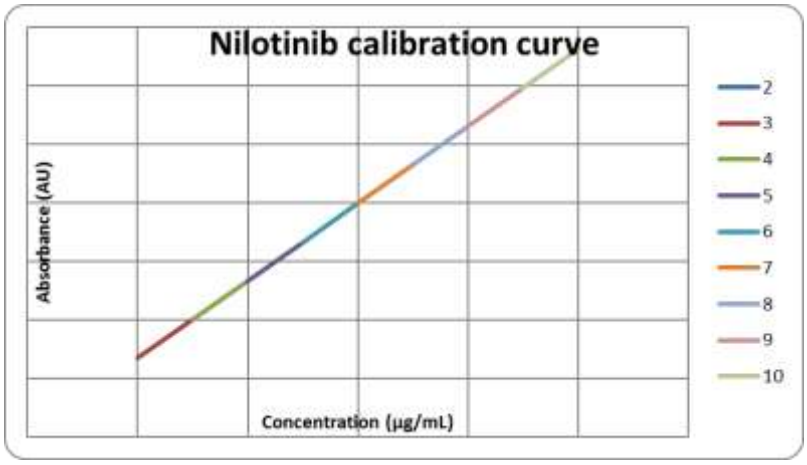

Fig 1: Nilotinib UV calibration data

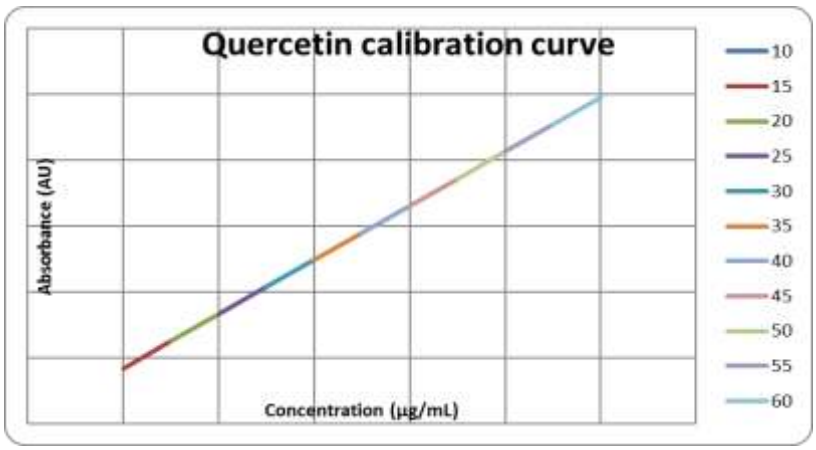

Fig 2: Quercetin UV calibration data.

3.3 FTIR compatibility assessment

The FTIR spectra of nilotinib, quercetin, Tween 80, GMO, Span 20 and the physical mixture were compared. The research interpretation reports retention of the principal characteristic bands without major disappearance or formation of new bands. The physical-mixture spectrum retained the nilotinib amide and C-F bands and the quercetin aryl-ether-associated band, supporting the absence of an obvious incompatibility signal under the conditions examined.

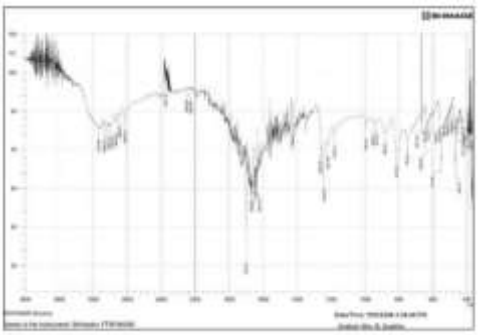

Fig 3: Nilotinib

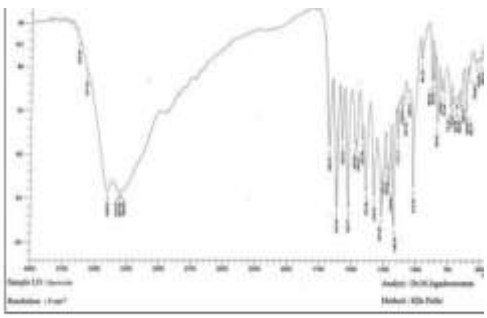

Fig 4: Quercetin

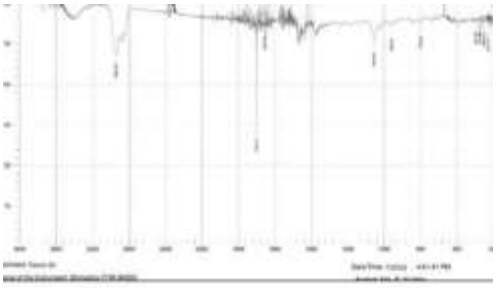

Fig 5: Tween 80

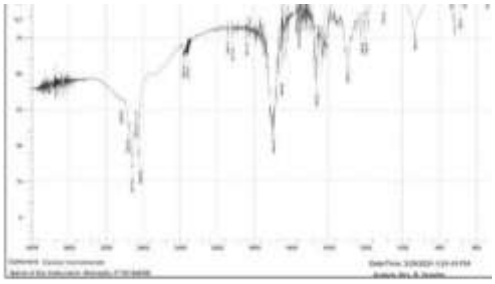

Fig 6: Glyceryl monostearate (GMO)

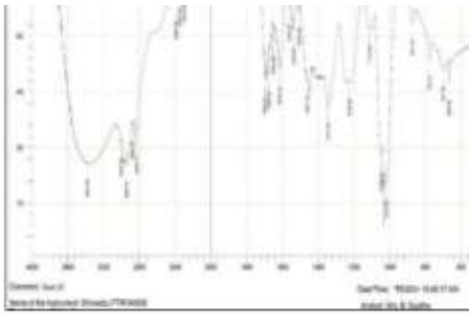

Fig 7: Span 20

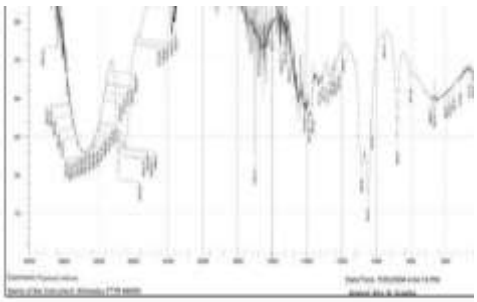

Fig 8: Physical mixture

The interpretation is limited to the qualitative comparison presented in the thesis. A full spectral overlay and a more detailed peak-assignment table are provided in the following section.

3.4 Characteristic FTIR bands

Table 2. FTIR peak positions (cm^{-1})

Functional group (cm^{-1})	Nilotinib	Quercetin	GMO	Tween 80	Span 20	Physical mixture
O-H stretching	3139.25	3406.05	3036.06	2946.36	2942.51	3132.50
C-H stretching	2828.70	-	2848.96	2355.16	2359.98	2775.66
C=O stretching	1659.80	-	1675.49	1655.94	1652.95	1679.09
-CH_3 bending	-	1461.94	1464.02	-	1461.13	1414.83
C-H bending	751.30	721.33	736.83	799.52	776.37	801.45
Aromatic C-H bending	-	1450.37	-	-	-	1505.49
Aryl ether	-	1319.22	-	-	-	1311.64
C=C bending	883.43	824.21	-	-	-	879.57
Amide stretching	1700.31	-	-	-	-	1700.31
C-F stretching	1259.80	-	-	-	-	1257.63

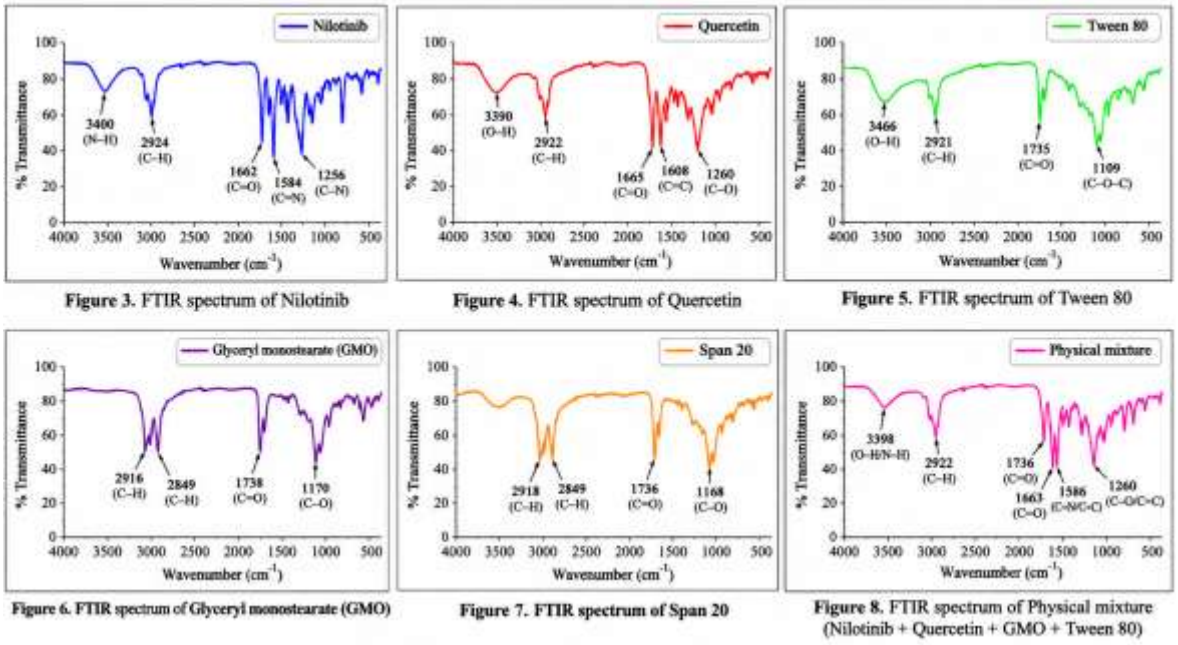

Figure 3. FTIR spectrum of Nilotinib

Figure 4. FTIR spectrum of Quercetin

Figure 5. FTIR spectrum of Tween 80

Figure 6. FTIR spectrum of Glyceryl monostearate (GMO)

Figure 7. FTIR spectrum of Span 20

Figure 8. FTIR spectrum of Physical mixture (Nilotinib + Quercetin + GMO + Tween 80)

Fig 9: Consolidated FTIR of ingredients (Generated image for additional clarity)

3.5 Physical appearance of trial batches

Table 3. Physical appearance of trial batches

Batch group	Composition	Observed appearance	Interpretation in research
T1-T2	4% GMO; Tween 80 1-1.5%	Slightly turbid dispersion	No visible phase separation reported
T3-T6	4-6% GMO; Tween 80 1-2%	Turbid dispersion	No visible phase separation reported
T7-T12	4-6% GMO; Span 20 1-2%	Initially turbid, then separated	Physical instability observed

The physical observations favored Tween 80 over Span 20 for the tested compositions. All Span 20 batches showed phase separation, preventing meaningful downstream comparison for those formulations.

3.6 Entrapment efficiency and drug content

Table 4. Entrapment efficiency and nilotinib content of the prepared SLN batches.

Batch	GMO (%)	Tween 80 (%)	Span 20 (%)	Entrapment efficiency (%)	Nilotinib content (%)
T1	4	1	-	48	98.19
T2	4	1.5	-	52	99.67
T3	4	2	-	64	99.18
T4	6	1	-	72	99.43
T5	6	1.5	-	86	98.36
T6	6	2	-	75	99.28
T7-T12	4 or 6	-	1-2	Separated	Not determined

Among the Tween 80 batches, entrapment efficiency increased from 48% in T1 to 86% in T5. Increasing GMO from 4% to 6% improved the reported entrapment values at comparable surfactant levels. At 6% GMO, increasing Tween 80 from 1.5% to 2% was associated with a decrease in entrapment efficiency from 86% to 75%. The highest reported nilotinib content was 99.67% in T2. T5 was selected as the lead formulation based on its highest reported entrapment efficiency and sustained release profile.

3.7 In-vitro drug-release profile

The release profiles showed an influence of lipid and surfactant concentration. T1 and T2 released almost all of both drugs within 6 h, whereas T5 showed the most prolonged profile among the reported batches.

Table 5. Cumulative in-vitro release of nilotinib (%).

Time (h)	T1	T2	T3	T4	T5	T6
0	0	0	0	0	0	0
1	45.93	38.56	39.57	27.75	23.71	25.12
3	70.14	67.55	56.39	40.65	33.88	36.07
6	99.09	99.52	65.78	52.51	42.69	49.23
9	-	-	88.03	64.36	51.55	60.93
12	-	-	99.51	72.85	61.16	68.56
16	-	-	-	83.53	74.47	78.96
20	-	-	-	90.24	83.66	85.89
24	-	-	-	99.43	93.55	99.16
30	-	-	-	-	99.92	-

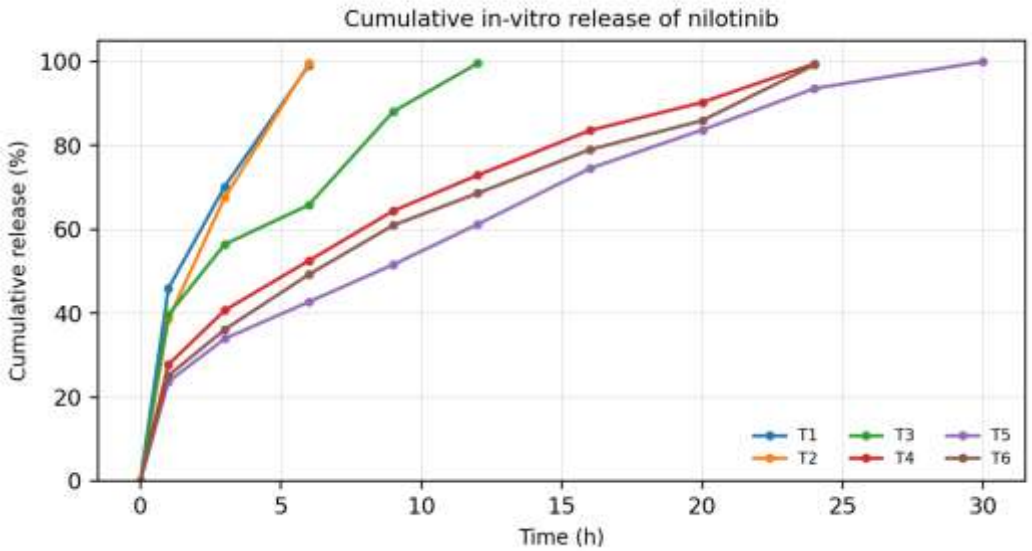

Fig 10: Cumulative in-vitro release of nilotinib from batches T1-T6.

3.7.1 Quercetin release and optimized-batch characterization

Table 6. Cumulative in-vitro release of quercetin (%)

Time (h)	T1	T2	T3	T4	T5	T6
0	0	0	0	0	0	0
1	49.98	42.67	32.10	30.80	22.83	21.04

3	81.10	74.56	48.01	40.95	31.13	30.39
6	99.99	99.64	63.67	53.01	40.75	38.03
9	-	-	80.96	64.10	51.28	47.45
12	-	-	98.97	77.41	62.56	60.01
16	-	-	-	85.07	70.71	70.50
20	-	-	-	94.72	77.34	84.62
24	-	-	-	99.31	88.86	99.62
30	-	-	-	-	99.17	-

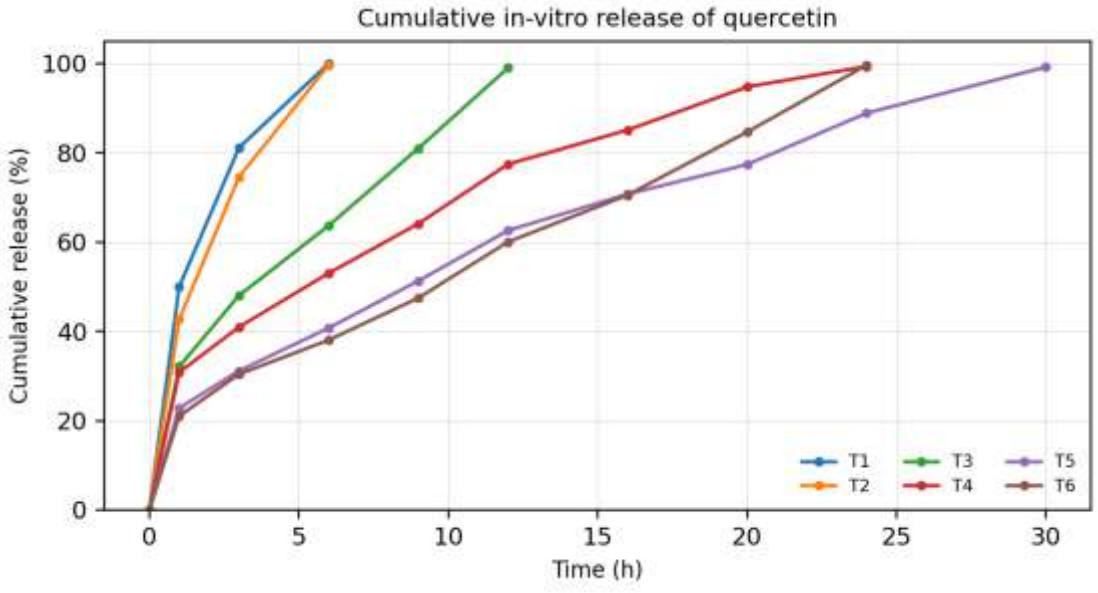

Fig 11: Cumulative in-vitro release of quercetin from batches T1-T6.

For T5, the reported cumulative release at 30 h was 99.92% for nilotinib and 99.17% for quercetin. The two profiles therefore showed broadly parallel sustained release in the selected batch.

Table 7. Particle-size distribution (278 nm; PDI 0.031)

Parameter	Result
Mean particle size (Z-average)	278 nm
Polydispersity index (PDI)	0.031

Table 8. Zeta-potential distribution (−32 mV)

Parameter	Result
Zeta potential	−32 mV

3.8 Surface morphology and in-vitro cytotoxicity

The SEM images in the thesis show predominantly rounded particles with smooth-looking surfaces, often present in clusters. The available micrograph is reproduced as Figure 13. The reported magnification was ×1000 at 5 kV; higher-magnification imaging would be needed to establish individual particle dimensions.

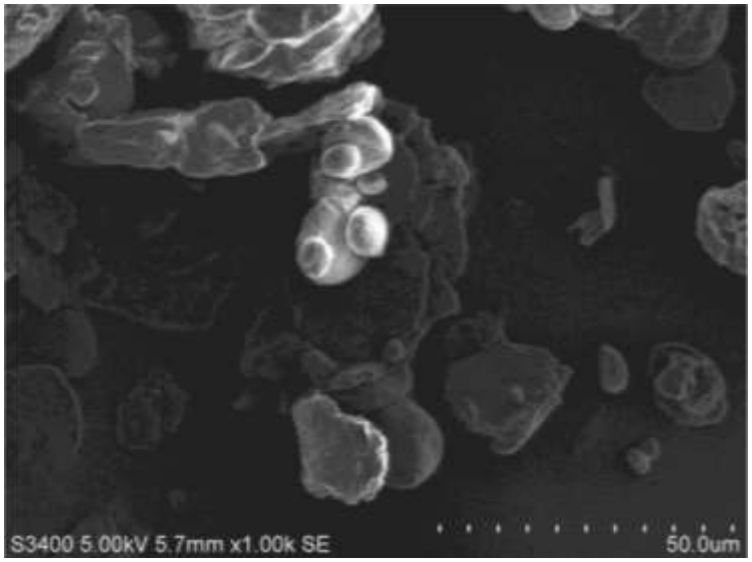

Fig 12: SEM micrograph of the nilotinib-quercetin SLN (×1000, 5 kV).

K562 cell viability decreased with increasing concentration for nilotinib, the free combination and the combination SLN. Quercetin alone showed a comparatively smaller reduction over the tested concentration range. The research table records 83.70% viability for the SLN at 5 µg/mL, compared with 72.16% for the free combination; at 10 µg/mL, the corresponding values were 2.31% and 5.21%.

Table 9. K562 cell viability (%) following treatment.

Concentration (µg/mL)	Nilotinib	Quercetin	Free combination	Combination SLN
5	38.37	99.99	72.16	83.7
10	10.32	99.95	5.21	2.31
15	2.11	93.73	0.17	0
20	0.12	80.31	0	0
25	0	74.97	0	0
30	0	61.28	0	0
35	0	58.14	0	0
40	0	43.02	0	0

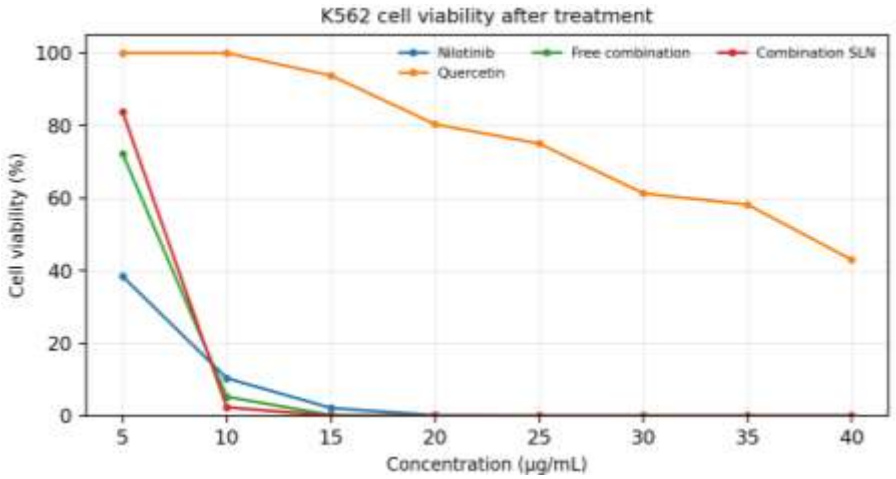

Fig 13: Concentration-dependent K562 cell viability for the four treatment groups.

3.9 IC50 comparison

Table10. Reported IC50 values in K562 cells.

Treatment	Reported IC50 (µg/mL)
Nilotinib	4.40
Quercetin	36.15
Nilotinib + quercetin (free combination)	3.80
Nilotinib + quercetin SLN	3.03

4. DISCUSSION

The preformulation findings were consistent with the limited aqueous solubility of nilotinib and quercetin and supported use of an organic solvent mixture during preparation and an acid-ethanol mixture for analytical measurements. The reported FTIR bands were largely retained in the physical mixture, with no major incompatibility signal identified by the qualitative peak comparison.

The surfactant comparison was a key formulation outcome. Tween 80 batches remained dispersed, while Span 20 batches separated. Within the Tween 80 series, T5 (6% GMO, 1.5% Tween 80) showed the highest reported entrapment efficiency (86%) and the most prolonged release. The selected batch had a mean particle size of 278 nm and a low PDI (0.031). The instrument output on thesis page 69 gives a mean zeta potential of −0.032 V, equivalent to −32 mV; this signed value is used here.

The reported IC50 for the co-loaded SLN (3.03 µg/mL) was lower than that for nilotinib alone (4.40 µg/mL) and the free combination (3.80 µg/mL). However, the viability data do not show a uniformly greater effect of the SLN at every concentration: at 5 µg/mL, viability was higher for the SLN than for the free combination. The data therefore support a preliminary difference in the reported IC50 estimates, but do not establish pharmacological synergy or a mechanism of enhanced cellular uptake.

5. CONCLUSION

Nilotinib and quercetin were co-formulated into GMO-based SLNs using hot homogenization followed by ultrasonication. Tween 80 produced dispersed batches, whereas Span 20 batches separated. T5 (6% GMO and 1.5% Tween 80) was the lead formulation based on the highest reported entrapment efficiency (86%) and sustained release to 30 h. The selected batch had a particle size of 278 nm, PDI of 0.031 and zeta potential of −32 mV. The reported IC50 in K562 cells was 3.03 µg/mL for the co-loaded SLN. These in-vitro findings warrant confirmation using adequately replicated assays, blank-carrier controls, stability testing and further preclinical evaluation.

6. REFERENCES

1. Sung H, Ferlay J, Siegel RL, Laversanne M, Soerjomataram I, Jemal A, et al. Global cancer statistics 2020: GLOBOCAN estimates of incidence and mortality worldwide for 36 cancers in 185 countries. CA Cancer J Clin. 2021;71(3):209-249.
2. Melo JV, Barnes DJ. Chronic myeloid leukaemia as a model of disease evolution in human cancer. Nat Rev Cancer. 2007;7(6):441-453.
3. Weisberg E, Manley PW, Breitenstein W, Brüggen J, Cowan-Jacob SW, Ray A, et al. Characterization of AMN107, a selective inhibitor of native and mutant Bcr-Abl. Cancer Cell. 2005;7(2):129-141.
4. Kantarjian H, Giles F, Wunderle L, Bhalla K, O'Brien S, Wassmann B, et al. Nilotinib in imatinib-resistant CML and Philadelphia chromosome-positive ALL. N Engl J Med. 2006;354(24):2542-2551.
5. Saglio G, Kim DW, Issaragrisil S, le Coutre P, Etienne G, Lobo C, et al. Nilotinib versus imatinib for newly diagnosed chronic myeloid leukemia. N Engl J Med. 2010;362(24):2251-2259.
6. Hochhaus A, Saglio G, Hughes TP, Larson RA, Kim DW, Issaragrisil S, et al. Long-term benefits and risks of frontline nilotinib vs imatinib for chronic myeloid leukemia in chronic phase: 5-year update of the randomized ENESTnd trial. Leukemia. 2016;30(5):1044-1054.
7. Plosker GL, Robinson DM. Nilotinib. Drugs. 2008;68(4):449-461.

8. Reyes-Farias M, Carrasco-Pozo C. The anti-cancer effect of quercetin: molecular implications in cancer metabolism. Int J Mol Sci. 2019;20(13):3177.
9. Vinayak M, Maurya AK. Quercetin loaded nanoparticles in targeting cancer: recent development. Anticancer Agents Med Chem. 2019;19(13):1560-1576.
10. Müller RH, Mäder K, Gohla S. Solid lipid nanoparticles (SLN) for controlled drug delivery—a review of the state of the art. Eur J Pharm Biopharm. 2000;50(1):161-177.
11. Mehnert W, Mäder K. Solid lipid nanoparticles: production, characterization and applications. Adv Drug Deliv Rev. 2001;47(2-3):165-196.
12. Wissing SA, Kayser O, Müller RH. Solid lipid nanoparticles for parenteral drug delivery. Adv Drug Deliv Rev. 2004;56(9):1257-1272.
13. Geszke-Moritz M, Moritz M. Solid lipid nanoparticles as attractive drug vehicles: composition, properties and therapeutic strategies. Mater Sci Eng C Mater Biol Appl. 2016;68:982-994.
14. Niazvand F, Orazizadeh M, Khorsandi L, Abbaspour M, Mansouri E, Khodadadi A. Effects of quercetin-loaded nanoparticles on MCF-7 human breast cancer cells. Medicina (Kaunas). 2019;55(4):114.
15. Mohamed JMM, Ahmad F, El-Sherbiny M, et al. Optimization and characterization of quercetin-loaded solid lipid nanoparticles for biomedical application in colorectal cancer. Cancer Nanotechnol. 2024;15:16.

ACKNOWLEDGEMENTS

The authors acknowledge the management and faculty of the Department of Pharmaceutics, JKK Munirajah Institute of Health Sciences College of Pharmacy, T.N. Palayam, for providing facilities and support.

CONFLICT OF INTEREST

The authors declare that they have no known competing financial interests or personal relationships that could have influenced the work reported in this manuscript.

AUTHORS' DECLARATION

We hereby declare that the manuscript entitled ***"Formulation and In-vitro Evaluation of Nilotinib and Quercetin Fused Nanoparticles for Enhanced Therapy of Myeloid Leukemia"*** represents original work. All authors have contributed to the preparation and development of the manuscript, have reviewed and approved the final version, and agree to its submission for publication. The manuscript has not been published previously and is not under consideration for publication elsewhere. All authors accept responsibility for the contents of the manuscript.

ETHICAL DECLARATION

The authors declare that this study did not involve human participants or human-derived biological samples. All experimental procedures were conducted in vitro. Therefore, ethical approval from an Institutional Ethics Committee was not applicable to this study.